Organic & Biomolecular Chemistry

Cite this: *Org. Biomol. Chem.*, 2012, **10**, 3219

www.rsc.org/obc

PAPER

Hydrogen tunnelling influences the isomerisation of some small radicals of interstellar importance. A theoretical investigation†

Tianfang Wang and John H. Bowie*

Received 15th December 2011, Accepted 6th February 2012
DOI: 10.1039/c2ob07102a

Hydrogen atom isomerisations within five radical systems (*i.e.*, $CH_3^{\cdot}NH/^{\cdot}CH_2NH$; $CH_3O^{\cdot}/^{\cdot}CH_2OH$; $^{\cdot}CH_2SH/CH_3S^{\cdot}$; $CH_3CO_2^{\cdot}/^{\cdot}CH_2CO_2H$; and $HOCH_2CH_2O^{\cdot}/HO^{\cdot}CHCH_2OH$) have been studied *via* quantum-mechanical hydrogen tunnelling through reaction barriers. The reaction rates including hydrogen tunnelling effects have been calculated for these gas phase reactions at temperatures from 300 K to 0 K using Wenzel–Kramers–Brillouin (WKB) and Eckart methods. The Eckart method has been found to be unsatisfactory for the last two systems listed above, because it significantly underestimates the width of the reaction barriers for the interconversions. The calculations at all-electron CCSD(T)/CBS level of theory indicate that the barriers for all reactions (forward and reverse) are greater than 100 kJ mol^{-1}, meaning that the chemical reactivity of the reactants is limited in the absence of hydrogen tunnelling. Hydrogen tunnelling, in some cases, enhance rates of reaction by more than 100 orders of magnitude at low temperature, and around 2 orders of magnitude at room temperature, compared to results obtained from canonical variational transition state theory. Tunnelling corrected reaction rates suggest that some of these isomerisation reactions may occur in interstellar media.

Introduction

The debate concerning the question as to whether the 'building-blocks' of life originated from interstellar space and/or by chemical reactions on prebiotic Earth has been attracting interest since the age of Aristotle.[1] To-date, about 170 molecules have been found in the interstellar medium[2–5] and there is evidence for the existence of far larger molecular species, the identities of which are currently unknown.[5] The search for biological molecules, for example amino acids, is ongoing.[6] Amino acids have been identified in some meteorites[7,8] and, arguably, in interstellar clouds.[9] It has been suggested that glycine may be formed in interstellar ice by the multistep process $^{\cdot}CH_2NH_2 + CO_2 + H \rightarrow NH_2CH_2CO_2H$,[10] while $^{\cdot}CH_2OH$ and $^{\cdot}CH_2SH$ have been proposed as reactants in the formation of serine and cysteine precursors in interstellar media.[11] Perhaps $^{\cdot}NH_2$ reacting with $^{\cdot}CH_2CN$, or $^{\cdot}CH_2NH_2$ coupling with $^{\cdot}CN$ may form the glycine precursor NH_2CH_2CN. Acetic acid (CH_3COOH) is a known interstellar molecule,[12] and it is possible that the reaction between $^{\cdot}NH_2$ and $^{\cdot}CH_2CO_2H$ can form glycine directly, while coupling of $NH_2^{\cdot}CHCN$ and $^{\cdot}CH_2CO_2H$ may form the aspartic acid precursor $NH_2CH(CH_2CO_2H)CN$.[11] The simplest two carbon sugar glycolaldehyde ($HOCH_2CHO$) has been detected in emission towards the Galactic centre source Sagittarius B2(N) by means of rotational transitions.[13,14] Several formation mechanisms of interstellar $HOCH_2CHO$ have been proposed, including the dimerisation of formaldehyde,[14] reactions between hydroxymethylene (:CHOH) and CH_2O,[15–18] CH_2O and H_3O^+,[19] and coupling reaction between $^{\cdot}CH_2OH$ and CH_2O.[18] It has been proposed that the reaction between $^{\cdot}CH_2OH$ and CH_2O yields $HOCH_2CH_2O^{\cdot}$ which then effects H transfer to form $HO^{\cdot}CHCH_2OH$ (barrier 117 kJ mol^{-1}), the key intermediate which reacts further with CH_2O to form C_6 sugars.[18] The interstellar reactions proposed above involve the radicals $^{\cdot}CH_2NH_2$, $^{\cdot}CH_2OH$, $^{\cdot}CH_2SH$, $^{\cdot}CH_2CO_2H$ and $HO^{\cdot}CHCH_2OH$; the key question is, are they stable or do they undergo H transfer to form isomers.

Department of Chemistry, The University of Adelaide, South Australia, 5005, Australia. E-mail: John.Bowie@adelaide.edu.au

† Electronic supplementary information (ESI) available: Section I Geometric structures and energies: Fig. S1 Geometries (in Å, deg) of minima and transition state structures optimised at AE-MP2/aug-cc-pVTZ level of theory; Table S1 Cartesian coordinates (in Å) of minima and transition state structures, optimised at AE-MP2(full)/aug-cc-pVTZ level of theory; Table S2 Zero-point vibrational energies (ZPVEs, calculated at AE-MP2/aVTZ, in hartree), single-point energies (calculated at AE-MP2/aVTZ, AE-CCSD(T)/aVnZ, n = D, T, Q, AE-CCSD(T)/CBS, in hartree) and relative energies (in kJ mol^{-1}); Table S3 Theoretical and experimental vibrational frequencies of minima in different isomerisations; Section II Tunnelling effects estimated by Eckart method: Table S4 Key parameters used in Eckart estimation; Fig. S2 Potential energy curve and rate constants for the isomerisation of $CH_3.NH$ to $^{\cdot}CH_2NH_2$; Fig. S3 Potential energy curve and rate constants for the isomerisation of $CH_3O.$ to $^{\cdot}CH_2OH$; Fig. S4 Potential energy curve and rate constants for the isomerisation of $^{\cdot}CH_2SH$ to $CH_3S^{\cdot}$; Fig. S5 Potential energy curve and rate constants for the isomerisation of $CH_3CO_2^{\cdot}$ to $^{\cdot}CH_2CO_2H$; Fig. S6 Potential energy curve and rate constants for the isomerisation of $HOCH_2CH_2O^{\cdot}$ to $HO{\cdot}CHCH_2OH^{\cdot}$]. See DOI: 10.1039/c2ob07102a

In this paper we investigate five reaction systems, all of which are of interstellar significance and all of which have substantial barriers for both the forward and reverse hydrogen transfers. These are (i) the 1,2-H rearrangements $CH_3NH^{\cdot}/{}^{\cdot}CH_2NH_2$; $CH_3O^{\cdot}/{}^{\cdot}CH_2OH$; ${}^{\cdot}CH_2SH/CH_3S^{\cdot}$; (ii) the 1,3-H rearrangement $CH_3CO_2{}^{\cdot}/{}^{\cdot}CH_2CO_2H$; and (iii) the 1,4-H rearrangement $HOCH_2CH_2O^{\cdot}/HO^{\cdot}CHCH_2OH$.

It has been shown that slow hydrogen tunnelling may influence exothermic reactions at low temperatures in interstellar media,[20–23] as the entropy factor plays no role near 0 K (*i.e.* $\Delta H = \Delta G$ at 0 K). For example, the product yields for the reactions of H with C_2H_2, C_2H_4, C_2H_6, CO and SiH_4 are indicative of hydrogen quantum mechanical tunnelling at low temperatures.[22] Similarly, the 1,2-H intramolecular insertions of :C(R)OH → RCHO (R = Ph, Me and H) involve intramolecular insertion of a carbene into an HO bond, and all three processes are dominated by H-tunnelling at low temperatures.[24–26] In marked contrast, the intermolecular carbene insertion of :CCCO into an NH bond of urea (NH_2CONH_2) to yield uracil, is not influenced by the large H-tunnelling effect at low temperatures because of the small rate constant of the reaction at low temperatures.[27]

It has been found that both H- and C-tunnelling effects [defined as the difference between the rate constant determined from classical transition-state theory and the overall rate (the rate constant determined by transition-state theory plus the tunnelling correction)] can be very large at low temperatures, but decrease with increasing temperature for intramolecular isomerisations involving H-transfer[28,29] and for intramolecular carbon rearrangement processes.[30–32] This behaviour seems at first sight to be counter-intuitive, but has been explained by the concept of vibrationally assisted tunnelling,[28] or thermally activated tunnelling.[32] At 0 K, only the ground vibrational level ($v = 0$) of the reaction mode takes part in tunnelling. As the temperature increases, the tunnelling reaction changes character from dominant ground-state tunnelling to dominant thermally activated tunnelling, with involvement of higher vibrational levels ($v = 1$, 2, 3, *etc.*). Thus with increasing temperature, this variation in the tunnelling mechanism effects a reduction in the tunnelling contribution ('through-barrier') towards an overall reaction rate as the non-tunnelling ('over-barrier') component increases.

This paper reports the results of a theoretical study of the five intramolecular H-transfer reaction systems described above, and demonstrates that H-tunnelling can influence reactions in both the forward and reverse directions. Temperatures may vary in different regions of the interstellar medium. It has been reported that (i) in dark and dense molecular clouds, the temperature is usually *ca.* 5–20 K in the cloud centre (which can be penetrated by cosmic and gamma radiation) but may be significantly higher in the outer regions of such clouds (due to penetration by ultraviolet, cosmic and gamma radiation and the influence of the solar wind); (ii) in diffuse clouds, temperatures may reach 100 K in the centre of the clouds; (iii) in interstellar water–ice systems, like water–ice comets heated mainly by ultraviolet radiation, the temperature may be ≥100 K, while in other water–ice systems the temperature may be higher; for example the water–ice rings of Saturn have a temperature of 240 K).[33,34] Such tunnelling, in principle, may be important in astrochemistry, and perhaps also for reactions operating under physiological conditions.[35–40] The relationship between the extent of H-tunnelling and temperature (between 0 and 300 K) is described for the five reaction systems.

Results and discussion

Because the energies of more stable structures for all isomerisations investigated here are not significantly lower than the corresponding isomers, it is possible that tunnelling may influence both forward and reverse reactions. Thus, rate constants for both forward and reverse reactions have been calculated. The forward reaction, defined as the thermal-dynamically favourable reaction direction, is the direction that hydrogen tunnelling may occur at low temperature. The reaction rates including hydrogen tunnelling effects have been calculated for these gas phase reactions at temperatures from 300 K to 0 K using Wenzel–Kramers–Brillouin (WKB) and Eckart methods. According to the description of the WKB method, the penetration integral [$\theta(\varepsilon)$, eqn (2), see computational methods section] and hence the tunnelling probability [$P(\varepsilon)$, eqn (3), computational methods section] is principally related to three factors at low temperature: these are (i) the square root of the effective mass, (ii) the square root of the difference between the overall barrier height and the collision energy, and (iii) the width of the barrier. Moreover, the barrier width (the distance the nuclei move in passing through the barrier) is more crucial than the barrier height in controlling the tunnelling reaction rate, because mathematically, the penetration integral (θ) scales linearly with the width of the barrier but only as the square root of the barrier height.

H-tunnelling can only take place for the reverse process above the vibrational level where the energy is higher than the product (the reactant in the forward direction). Thus H-tunnelling for the reverse process will be low at low temperatures. As the temperature increases, the population of higher vibrational levels will increase, which may lead to an increase of H-tunnelling for the reverse process.

1. $CH_3{}^{\cdot}NH$ and ${}^{\cdot}CH_2NH_2$

A possible interstellar synthesis of the glycine precursor aminoacetonitrile (NH_2CH_2CN), involves the barrierless reaction between ${}^{\cdot}CH_2NH_2$ and ${}^{\cdot}CN$.[11] The cyanide radical is a known interstellar molecule, whereas ${}^{\cdot}CH_2NH_2$ has not been identified in interstellar molecular clouds.[5] However, methylamine (CH_3NH_2) is an interstellar molecule,[5] and it has been proposed that cosmic rays can convert methylamine to both ${}^{\cdot}CH_2NH_2$ and $CH_3{}^{\cdot}NH$.[10] The radical ${}^{\cdot}CH_2NH_2$ is stable at low pressure ($\sim 10^{-4}$ Torr) at room temperature for the microsecond time scale.[11] However, (i) is ${}^{\cdot}CH_2NH_2$ stable at low temperature, and (ii) does quantum-mechanical H-tunnelling influence interconversion of ${}^{\cdot}CH_2NH_2$ and $CH_3{}^{\cdot}NH$ at low temperature?

The canonical variational transition state theory (CVT) rate (k_{CVT}) for the forward reaction is slow because of the high barrier (see Fig. 1, calculated at AE-CCSD/CBS//AE-MP2/aVTZ level of theory, with geometry, energy and vibrational frequency comparison data recorded as ESI Fig. S1,† and Tables S1 to S3†), *e.g.*, 3.36×10^{-148} s^{-1} at 50 K and 1.67×10^{-14} s^{-1} at 300 K. However, the actual reaction rate is affected by hydrogen tunnelling as shown in Fig. 2. The reaction pathway (Fig. 2)

connecting the transition state to $CH_3{}^{\cdot}NH$ and $^{\cdot}CH_2NH_2$ through the hyperspace of the 12 vibrational degrees of freedom is adopted as the tunnelling route, the forward reaction mode has a harmonic vibrational frequency (ω_0) of 986 cm^{-1}; and collision energy (ε) at 0 K is set equivalent to the zero-point vibrational energy (ZPVE) of the reaction mode ($\omega_0/2$). The WKB rate calculations were carried out using the potential energy expression obtained by the polynomial fitting approach (*cf.*, the red curve in Fig. 2a), which closely represents the potential energy surface. The corrected rate results are shown in Fig. 2b. The results of the Eckart method [ESI (Fig. S2†)] are qualitatively in agreement with the WKB tunnelling estimation.

Table 1 lists results at 50 and 300 K. The WKB rate constant of the forward reaction ($k_{WKB} = 6.42 \times 10^{-14}$) at 50 K results in a half-life of 3.42×10^5 years [calculated according to eqn (6)], while at 300 K ($k_{WKB} = 3.01 \times 10^{-10}$) the half-life decreases to 73 years. At low temperature, even though k_{WKB} is greatly enhanced in comparison with k_{CVT} by more than 130 orders of magnitude, the overall k_{WKB} is still very small. This yields a half-life of $CH_3{}^{\cdot}NH$ that is so long that the reaction is not feasible in the interstellar medium at low temperature. The reverse reaction rate is extremely small at low temperature (see Fig. 2b and Table 1), and increases with increasing temperature, but it is still about 5 orders of magnitude smaller than the forward rate at 300 K, which means that the reverse reaction is negligible within this temperature regime.

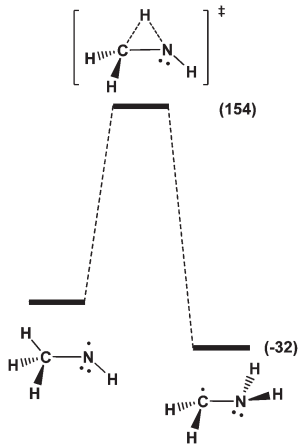

Fig. 1 Reaction coordinate diagram for $CH_3{}^{\cdot}NH$ to $^{\cdot}CH_2NH_2$ at AE-CCSD(T)/CBS//AE-MP2/aVTZ level of theory at 0 K, ΔH in kJ mol^{-1}.

2. $CH_3O^{\cdot}$ and $^{\cdot}CH_2OH$

$^{\cdot}CH_2OH$ has been proposed as a reactant in forming glycolaldehyde ($HOCH_2CHO$),[18] the proto two-carbon sugar, and has been detected in emission towards the Galactic centre source Sagittarius B2(N) by means of multimeter-wave rotational transitions.[13,14] The methoxy radical ($CH_3O^{\cdot}$) is also known to be a stable interstellar molecule.[41] Both $CH_3O^{\cdot}$ and $^{\cdot}CH_2OH$ are stable at room temperature for the microsecond duration of a neutralisation–reionisation mass-spectrometry process, and no isomerisation between them has been detected during this timeframe when energised.[18] What is the situation at low temperature and does hydrogen tunnelling influence isomerisation? The relative energy at 0 K for the unimolecular isomerisation of $CH_3O^{\cdot}$ to $^{\cdot}CH_2OH$ calculated at the AE-CCSD(T)/CBS//AE-MP2/aVTZ level of theory is shown in Fig. 3, in which $CH_3O^{\cdot}$ requires 125 kJ mol^{-1} to surmount the barrier and reach $^{\cdot}CH_2OH$ at −42 kJ mol^{-1}. Full geometry, energy and vibrational frequency comparison data are recorded as ESI (Fig. S1, Tables S1 to S3†). The quartet state of $CH_3O^{\cdot}$ is not stable at the AE-MP2/aVTZ level of theory, with an imaginary frequency of 159*i*; so only the potential surface of the doublet isomerisations is investigated

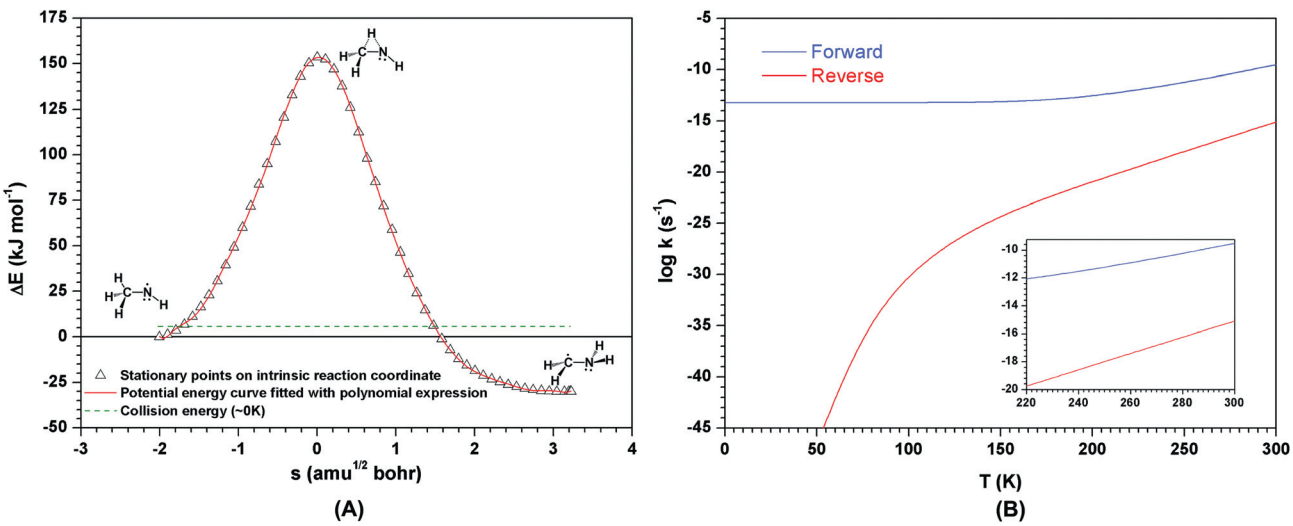

Fig. 2 Potential energy curve and rate constants for the isomerisation of $CH_3{}^{\cdot}NH$ to $^{\cdot}CH_2NH_2$. (a) Along the intrinsic reaction coordinate (open triangles), the geometric structures and zero-point vibrational corrections were calculated at the AE-MP2/aVTZ level of theory, and final energies were determined from AE-CCSD(T)/aVQZ single points at the stationary points. The red curve is the polynomial fitting of the intrinsic reaction coordinate, and this is required for the calculation of k_{WKB}; (b) temperature dependence of WKB tunnelling corrected rate constants for both forward and reverse reactions, with high temperature region (220–300 K) enlarged.

Table 1 Tunnelling effects[a] at 50 and 300 K for isomerisation of $CH_3{}^{\cdot}NH$ and $^{\cdot}CH_2NH_2$

		Forward			Reverse		
Isomerisation	T (K)	k_{CVT} (s^{-1})	k_{WKB} (s^{-1})	Half-life (WKB)	k_{CVT} (s^{-1})	k_{WKB} (s^{-1})	Half-life (WKB)
$CH_3{}^{\cdot}NH$ to $^{\cdot}CH_2NH_2$	50	3.36×10^{-148}	6.42×10^{-14}	3.42×10^{5} years	1.44×10^{-179}	2.99×10^{-47}	7.34×10^{38} years
	300	1.67×10^{-14}	3.01×10^{-10}	73.0 years	3.42×10^{-19}	7.99×10^{-16}	2.75×10^{7} years

[a] Calculated at the AE-CCSD(T)/aVQZ//AE-MP2/aVTZ level of theory.

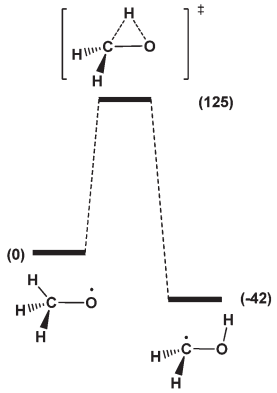

Fig. 3 Reaction coordinate diagram for $CH_3O^{\cdot}$ to $^{\cdot}CH_2OH$ at the AE-CCSD(T)/CBS//AE-MP2/aVTZ level of theory at 0 K. ΔH in kJ mol^{-1}.

here. Previous kinetic studies[42] have proposed the standard heat of formation for $CH_3O^{\cdot}$ and $^{\cdot}CH_2OH$ to be 21 and −13 kJ mol^{-1}; in this work, the calculation leads to $\Delta_f H^0_{298K}$ ($CH_3O^{\cdot}$) = 27 kJ mol^{-1} and $\Delta_f H^0_{298\ K}$ ($^{\cdot}CH_2OH$) = −13 kJ mol^{-1}.

The intrinsic reaction coordinate constructs a hyperspace of 9 vibrational degrees of freedom as the tunnelling route, and the vibrational 'reaction' mode of $CH_3O^{\cdot}$ that corresponds to the transition state has a harmonic frequency of ω_0 = 978 cm^{-1}. Fig. 4a shows the polynomial fitted potential energy surface, and the theoretical analysis yields the rate constants at different temperatures as displayed in Fig. 4b for the forward and reverse reactions. Rate and half-life data at 50 and 300 K are listed in Table 2.

The WKB rate constant for the forward reaction (k_{WKB} = 4.44 × 10^{-8} s^{-1}) at 50 K corresponds to the half-life of $CH_3O^{\cdot}$ of about 180.6 days (see Table 2), and this value stays nearly

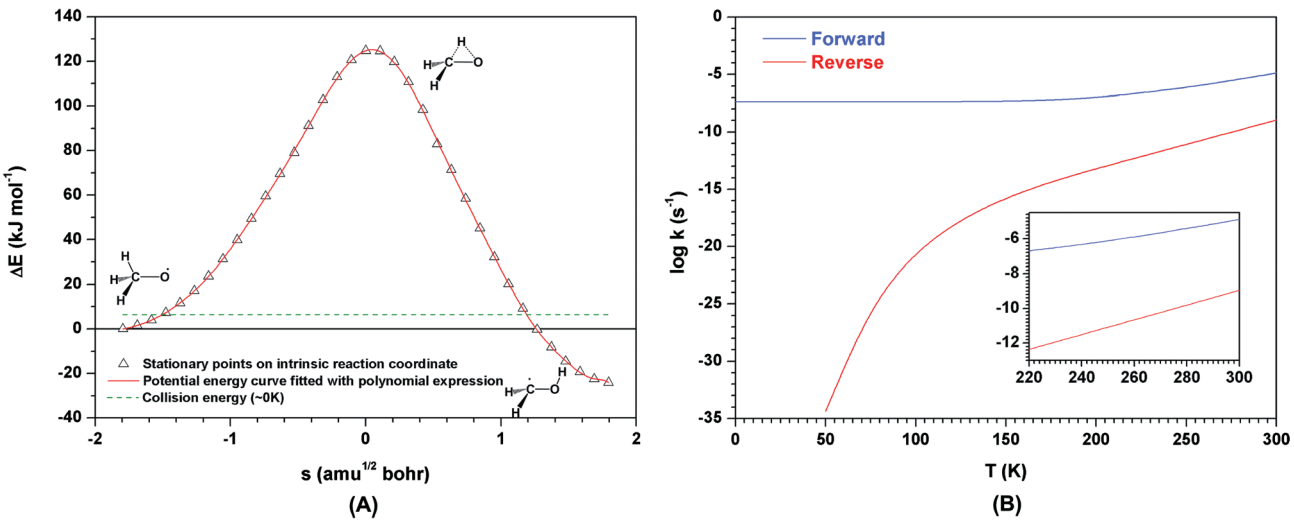

Fig. 4 Potential energy curve and rate constants for the isomerisation of $CH_3O^{\cdot}$ to $^{\cdot}CH_2OH$. (a) Along the intrinsic reaction coordinate (open triangles), the geometric structures and zero-point vibrational corrections were calculated at the AE-MP2/aug-cc-pVTZ level of theory, and final energies were determined from AE-CCSD(T)/aug-cc-pVQZ single points at the stationary points. The red curve is the polynomial fitting of the intrinsic reaction coordinate. (b) Temperature dependence of WKB tunnelling corrected rate constants for both forward and reverse reactions, with high temperature region (220–300 K) enlarged.

Table 2 Tunnelling effects[a] at 50 and 300 K for isomerisation of $CH_3O^{\cdot}$ and $^{\cdot}CH_2OH$

		Forward			Reverse		
Isomerisation	T (K)	k_{CVT} (s^{-1})	k_{WKB} (s^{-1})	Half-life (WKB)	k_{CVT} (s^{-1})	k_{WKB} (s^{-1})	Half-life (WKB)
$CH_3O^{\cdot}$ to $^{\cdot}CH_2OH$	50	3.04×10^{-118}	4.44×10^{-8}	180.6 day	1.00×10^{-143}	4.49×10^{-35}	4.89×10^{26} years
	300	2.43×10^{-9}	1.32×10^{-5}	14.6 h	1.18×10^{-13}	1.12×10^{-9}	19.6 years

[a] Calculated at the AE-CCSD(T)/aVQZ//AE-MP2/aVTZ level of theory.

constant up to 150 K (see Fig. 4b), suggesting that H-tunnelling effects interconversion of $CH_3O^{\cdot}$ to $^{\cdot}CH_2OH$ at a low rate within this temperature range, and the H-tunnelling mainly involves ground and lower vibrational levels (thermally activated mechanism is limited). The reverse reaction basically does not occur in the temperature regime <150 K. At 300 K the overall rate for the forward reaction is more favourable with the half-life of $CH_3O^{\cdot}$ now only 14.6 h. The reverse rate constant is around 1/10 000th of the forward rate constant at 300 K, with the half life of $^{\cdot}CH_2OH$ at this temperature being 19.6 years. This means that the formation of $^{\cdot}CH_2OH$ from $CH_3O^{\cdot}$ is the more favourable reaction over the temperature range 0–300 K. Considering the life of molecular clouds ($\sim 10^7$ years[43,44]), this result suggests an acceptable formation pathway of $^{\cdot}CH_2OH$. Results from the Eckart method are similar (see Fig. S3†).

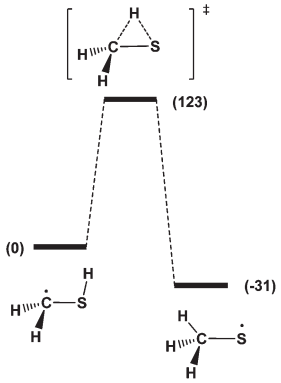

Fig. 5 Reaction coordinate diagram for $^{\cdot}CH_2SH$ to $CH_3S^{\cdot}$ at the AE-CCSD(T)/CBS//AE-MP2/aVTZ level of theory at 0 K. ΔH in kJ mol^{-1}.

3 $^{\cdot}CH_2SH$ and $CH_3S^{\cdot}$

It has been suggested that the mercaptomethyl radical ($^{\cdot}CH_2SH$) may be involved in the radical–radical coupling reaction [$NH_2{}^{\cdot}CHCN + {}^{\cdot}CH_2SH \rightarrow NH_2CH(CH_2SH)CN$] to form the nitrile precursor of cysteine.[11] The neutralisation/reionisation mass spectra of $^{-}CH_2SH$ and CH_3S^{-} confirm that both $^{\cdot}CH_2SH$ and $CH_3S^{\cdot}$ are stable for at least a microsecond at room temperature.[11,45] The ground state of $^{\cdot}CH_2SH$ is the doublet, with the quartet structure unstable at the AE-MP2/aVTZ level of theory.

The isomerisation reaction between $^{\cdot}CH_2SH$ and $CH_3S^{\cdot}$ is different from that of $CH_3O^{\cdot}/{}^{\cdot}CH_2OH$, with $CH_3S^{\cdot}$ being more stable than $^{\cdot}CH_2SH$ by 31 kJ mol^{-1} (see Fig. 5) at 0 K. This can be attributed to the relative electron affinities of carbon (1.26 eV),[46] oxygen (+1.46 eV)[46] and sulfur (2.08 eV).[46] The heat of formation of $CH_3S^{\cdot}$ at 0 K ($\Delta_f H_{0\ K}$) is calculated to be 135.9 kJ mol^{-1}, in good agreement with values determined from photodissociation spectroscopy (129.83 ± 1.70 kJ mol^{-1})[47] and reaction kinetic measurements (131.52 ± 2.23 kJ mol^{-1});[48] $\Delta_f H^0_{298\ K}(CH_3S^{\cdot}) = 128.5$ kJ mol^{-1}, and it is consistent with the reported values (*e.g.*, 124.6 ± 1.84,[48] 123.0 ± 8.8,[49] 131.4 ± 8.4,[50] and 127.6 ± 8.4[51] kJ mol^{-1}). The barrier for the reaction is 123 kJ mol^{-1} at the AE-CCSD(T)/CBS//AE-MP2/aVTZ level of theory. Full geometry and energy data, together with vibrational frequencies are recorded in Fig. S1 and Tables S1–S3.†

The tunnelling analysis was performed using both WKB and Eckart estimations based on the intrinsic reaction coordinate determined at the AE-CCSD(T)/aVQZ//AE-MP2/aVTZ level of theory. For the forward reaction, the reaction mode vibrational frequency is 821 cm^{-1}. The WKB results are summarised in Fig. 6 with Eckart results in Fig. S4,† and the rate constants estimated by both methods are in satisfactory accordance (see Fig. 6b and S4b†). Results at two temperatures are summarised in Table 3. At 50 K, k_{WKB} (2.86×10^{-6} s^{-1}) for the forward reaction is more than 80 orders of magnitude greater than that

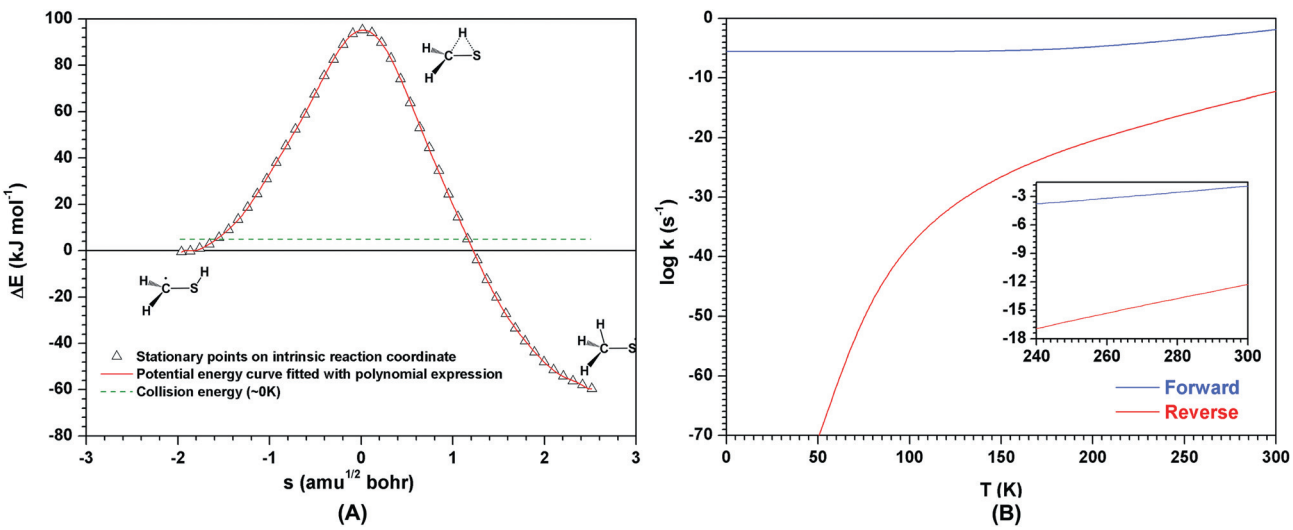

Fig. 6 Potential energy curve and rate constants for the isomerisation of $^{\cdot}CH_2SH$ to $CH_3S^{\cdot}$. (a) Along the intrinsic reaction coordinate (open triangles), the geometric structures and zero-point vibrational corrections were calculated at the AE-MP2/aVTZ level of theory; final energies were determined from AE-CCSD(T)/aVQZ single points at the stationary points. The red curve is the polynomial fitting of the intrinsic reaction coordinate; (b) temperature dependence of WKB tunnelling corrected rate constants for both forward and reverse reactions, with high temperature region (240–300 K) enlarged.

Table 3 Tunnelling effects[a] at 50 and 300 K for isomerisation of $^{\cdot}CH_2SH$ and $CH_3S^{\cdot}$

		Forward			Reverse		
Isomerisation	T (K)	k_{CVT} (s^{-1})	k_{WKB} (s^{-1})	Half-life (WKB)	k_{CVT} (s^{-1})	k_{WKB} (s^{-1})	Half-life (WKB)
$^{\cdot}CH_2SH$ to $CH_3S^{\cdot}$	50	4.76×10^{-88}	2.86×10^{-6}	67.2 h	9.97×10^{-150}	3.00×10^{-71}	7.33×10^{62} years
	300	2.92×10^{-4}	1.29×10^{-2}	53.7 s	2.49×10^{-14}	5.70×10^{-13}	3.86×10^{4} years

[a] Calculated at the AE-CCSD(T)/aVQZ//AE-MP2/aVTZ level of theory.

evaluated using the canonical variational TST approach, and the H-tunnelling effect contributes markedly to the overall reaction rate. The H-tunnelling effect for the reverse reaction is large at 50 K but because k_{WKB} is so small, no reaction occurs (see Table 3). This indicates that (i) $^{\cdot}CH_2SH$ readily converts to $CH_3S^{\cdot}$ at low temperature and (ii) the reverse reaction does not occur under these conditions. The short half-life (53.7 s) for forward reaction at 300 K shows that the isomerisation is facile at this temperature, whereas the reverse reaction is still negligible. Thus, $^{\cdot}CH_2SH$ is not stable in interstellar media over 0 to 300 K, and is unlikely to be involved in the formation of the cysteine precursor $NH_2CH(CH_2SH)CN$ under these reaction conditions.

4. $CH_3CO_2^{\cdot}$ and $^{\cdot}CH_2CO_2H$

The radical $^{\cdot}CH_2CO_2H$ may be involved in the syntheses of glycine and an aspartic acid precursor in interstellar media. Acetic acid (CH_3COOH) has been identified in the Sgr B2 Large Molecule Heimat,[12] and H-abstraction may form both $CH_3CO_2^{\cdot}$ and $^{\cdot}CH_2COOH$. $CH_3CO_2^{\cdot}$ has been confirmed to be stable at low pressures in the gas phase at room temperature.[52] Does H-tunnelling influence isomerisation between these two radicals at low temperatures?

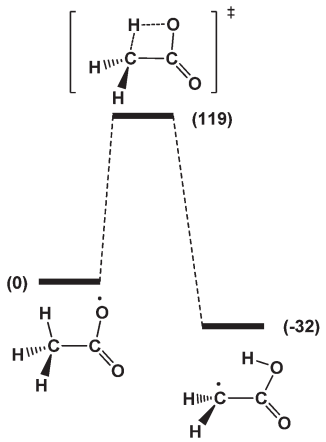

Fig. 7 Reaction coordinate diagram for the isomerisation of $CH_3CO_2^{\cdot}$ and $^{\cdot}CH_2CO_2H$ at the AE-CCSD(T)/CBS//AE-MP2/aVTZ level of theory at 0 K. ΔH in kJ mol^{-1}.

Since the doublet-quartet gap for $CH_3CO_2^{\cdot}$ is 417 kJ mol^{-1} at the AE-CCSD(T)/aVTZ//AE-MP2/aVTZ level of theory, only the doublet potential surface has been considered in this study. The reaction coordinate diagram at 0 K is shown in Fig. 7. The

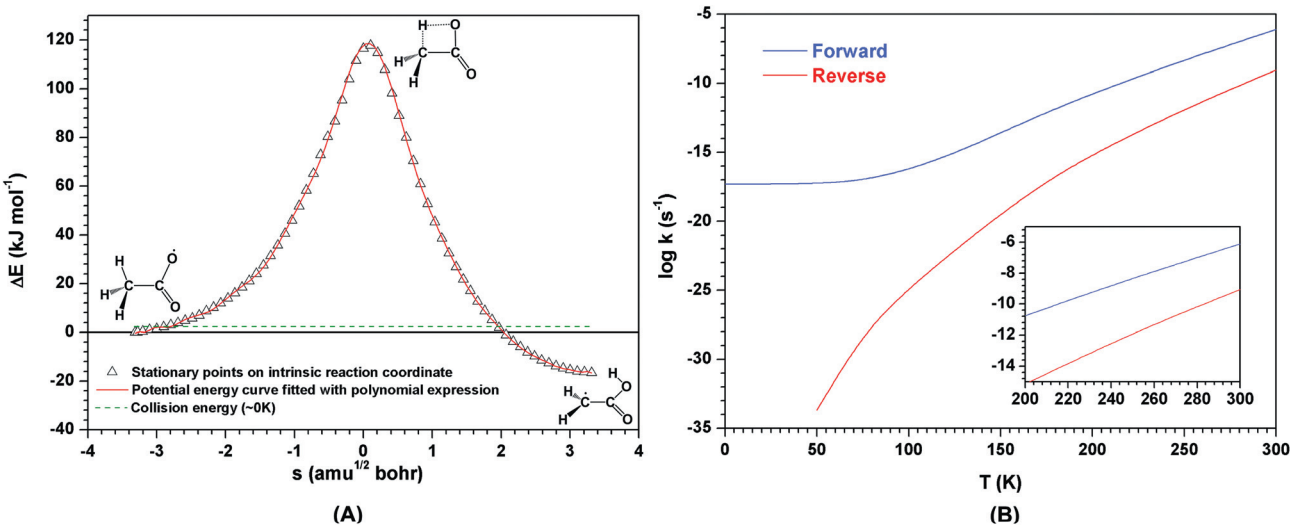

Fig. 8 Potential energy curves for the isomerisation of $CH_3CO_2^{\cdot}$ and $^{\cdot}CH_2CO_2H$. (a) Along the intrinsic reaction coordinate (open triangles), the geometric structures and zero-point vibrational corrections were calculated at the AE-MP2/aVTZ level of theory, and final energies were determined from AE-CCSD(T)/aVTZ single points at the stationary points. The red curve is the polynomial fitting of the intrinsic reaction coordinate; (b) temperature dependence of WKB tunnelling corrected rate constants for both forward and reverse reactions, with high temperature region (200–300 K) enlarged.

Table 4 Tunnelling effects[a] at 50 and 300 K for isomerisation of $CH_3CO_2^{\cdot}$ and $^{\cdot}CH_2CO_2H$

		Forward			Reverse		
Isomerisation	T (K)	k_{CVT} (s^{-1})	k_{WKB} (s^{-1})	Half-life (WKB)	k_{CVT} (s^{-1})	k_{WKB} (s^{-1})	Half-life (WKB)
$CH_3CO_2^{\cdot}$ and $^{\cdot}CH_2CO_2H$	50	1.74×10^{-109}	4.91×10^{-18}	4.48×10^{9} years	1.00×10^{-126}	2.06×10^{-34}	1.07×10^{26} years
	300	6.71×10^{-8}	7.86×10^{-7}	245.0 h	4.45×10^{-10}	8.89×10^{-10}	24.7 years

[a] Calculated at the AE-CCSD(T)/aVTZ//AE-MP2/aVTZ level of theory.

barrier for the forward reaction is 119 kJ mol^{-1}, and $^{\cdot}CH_2CO_2H$ is the more stable isomer by 32 kJ mol^{-1}. Full geometry and energy data are recorded in Fig. S1, Tables S1 and S2.†

The intrinsic reaction potential energy calculations and fitted polynomial expression plot are shown in Fig. 8a, where good correspondence is obtained. The rate results of the WKB calculations are provided in Fig. 8b, while rate and half-life data at 50 and 300 K are summarised in Table 4. Forward and reverse k_{WKB} are small at 50 K, a function of the significant width at the bottom of the potential barrier. Thus, at cryogenic temperatures, $^{\cdot}CH_2CO_2H$ is not formed from $CH_3CO_2^{\cdot}$, and vice versa. At room temperature, the forward k_{WKB} (7.86×10^{-7} s^{-1}, compared to $k_{CVT} = 6.71 \times 10^{-8}$ s^{-1}) corresponds to a half-life 245 hours, which is significantly shorter than that of reverse process. Thus $CH_3CO_2^{\cdot}$ is stable at low temperatures, with isomerism in the forward direction more favourable at room temperature. The Eckart method underestimates the width of the interconversion barrier, and, as a consequence, overestimates the overall rate constant in comparison with k_{WKB} (see ESI Fig. S5†).

5. $HOCH_2CH_2O^{\cdot}$ and $HO^{\cdot}CHCH_2OH$

It has been recently proposed that (i) $^{\cdot}CH_2OH/CH_2O$ addition to form $HO^{\cdot}CHCH_2OH$ may be a key reaction in the interstellar formation of sugars, and (ii) the least favourable step in this sequence is the isomerisation of $HOCH_2CH_2O^{\cdot}$ to $HO^{\cdot}CHCH_2OH$ which has a barrier of 120 kJ mol^{-1} at the CCSD(T)/6-311++G(3df,2p)//MP2/6-311++G(3df,2p) level of theory.[18] Perhaps H-tunnelling can assist this isomerisation?

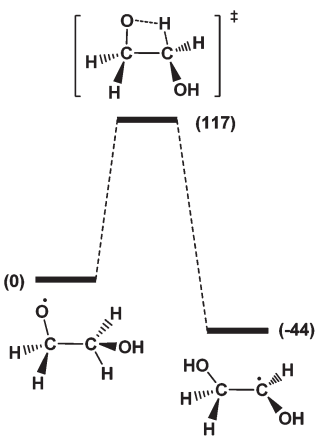

Fig. 9 Reaction coordinate diagram for $HOCH_2CH_2O^{\cdot}$ and $HO^{\cdot}CHCH_2OH$ isomerisations at the AE-CCSD(T)/CBS//AE-MP2/aVTZ level of theory at 0 K. ΔH in kJ mol^{-1}.

The doublet potential surface has been studied because quartet $HOCH_2CH_2O^{\cdot}$ is unstable at the AE-MP2/aVTZ level of theory. The relative enthalpies of the reaction at 0 K calculated at the AE-CCSD(T)/CBS//AE-MP2/aVTZ level of theory are shown in Fig. 9 with full geometry and energy data recorded in Fig. S1 and Tables S1 and S2.† The forward reaction is exothermic by 44 kJ mol^{-1} and there is a barrier of +117 kJ mol^{-1} for the isomerisation of $HOCH_2CH_2O^{\cdot}$ to $HO^{\cdot}CHCH_2OH$.

The intrinsic reaction pathway is recorded in Fig. 10a (open triangles), together with the polynomial fitting curve. The bottom of the barrier is broader than those of any of the reaction coordinates of the other systems discussed above. The fitting curve satisfactorily represents the intrinsic reaction coordinate, whereas the Eckart method is not appropriate in this case since it narrows the barrier (see Fig. S6†). The WKB rate constants are shown in Fig. 10b and summarised in Table 5. Although the H-tunnelling effect is very large for both forward and reverse reactions at low temperatures, the WKE rate constants remain small so the overall tunnelling influence is negligible. At room temperature the half-life of $HOCH_2CH_2O^{\cdot}$ (40.3 days) is much shorter than that of $HO^{\cdot}CHCH_2OH$ (2.36×10^5 years), suggesting slow forward isomerisation under these conditions.

Summary and conclusions

Computational results for reactions at 50 and 300 K are collected in Table 6. In summary:

(1) In all cases, the exothermicity of the H rearrangements are of the order of 30–40 kJ mol^{-1} and H-tunnelling effects occur for both forward and reverse reactions.

(2) H-tunnelling influences the isomerisation of $^{\cdot}CH_2SH$ most significantly, where the half-lives of 67.2 hours and 53.7 seconds at 50 and 300 K respectively allow $^{\cdot}CH_2SH$ to interconvert to $CH_3S^{\cdot}$. The reverse reaction basically does not occur over 0 to 300 K temperature range. Thus $^{\cdot}CH_2SH$ should readily isomerise to $CH_3S^{\cdot}$ in interstellar media.

(3) H-tunnelling within the $CH_3O^{\cdot}$ to $^{\cdot}CH_2OH$ barrier enhances the formation of $^{\cdot}CH_2OH$ at both low and room temperatures (half-lives of $CH_3O^{\cdot}$ are 180.6 days and 14.6 hours at 50 and 300 K respectively). The reverse reaction does not occur within 0–300 K. The forward reaction will be slow, but significant in, for example, a molecular cloud with a lifetime of 10^7 years.

(4) The systems $CH_3CO_2^{\cdot}/^{\cdot}CH_2CO_2H$ and $HOCH_2CH_2O^{\cdot}/HO^{\cdot}CHCH_2OH$ exhibit large tunnelling effects at 50 K for both forward and reverse reactions but because of the small k_{WKB} rates, interconversion is not observed at this temperature. Much reduced H-tunnelling effects accompany these reactions at

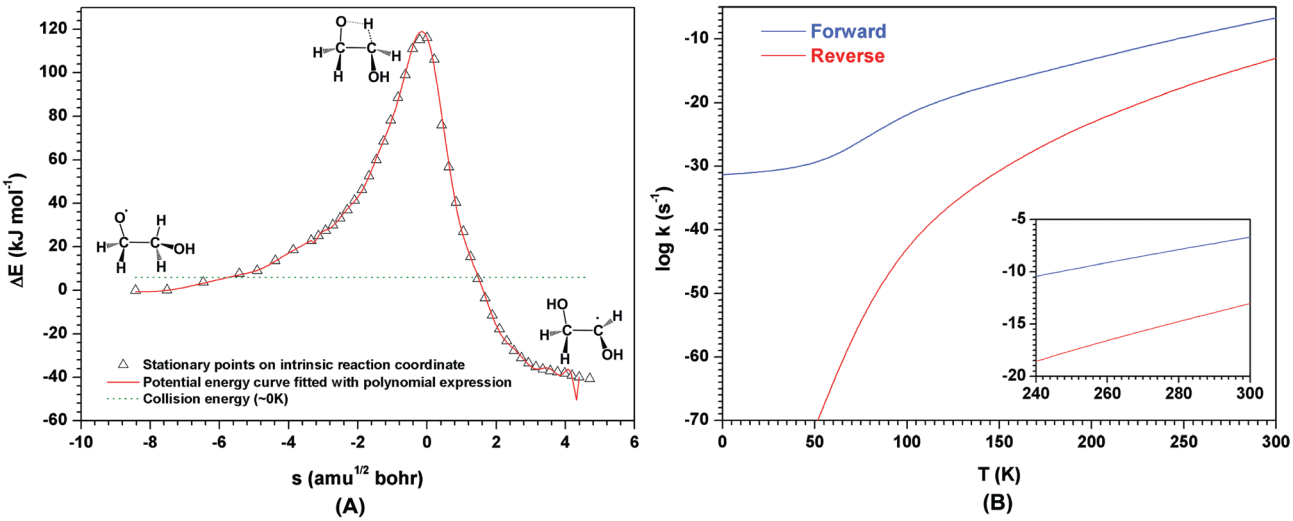

Fig. 10 Potential energy curves for the isomerisation of $HOCH_2CH_2O^{\cdot}$ and $HO^{\cdot}CHCH_2OH$. Along the intrinsic reaction coordinate (open triangles), the geometric structures and zero-point vibrational corrections were calculated at the AE-MP2/aVTZ level of theory. The red curve is the polynomial fitting of the intrinsic reaction coordinate; (b) temperature dependence of WKB H-tunnelling corrected rate constants for both forward and reverse reactions, with high temperature region (240–300 K) enlarged.

Table 5 Tunnelling effects[a] at 50 and 300 K for isomerisation of $HOCH_2CH_2O^{\cdot}$ and $HO^{\cdot}CHCH_2OH$

		Forward			Reverse		
Isomerisation	T (K)	k_{CVT} (s^{-1})	k_{WKB} (s^{-1})	Half-life (WKB)	k_{CVT} (s^{-1})	k_{WKB} (s^{-1})	Half-life (WKB)
$HOCH_2CH_2O^{\cdot}$ and $HO^{\cdot}CHCH_2OH$	50	2.79×10^{-108}	4.42×10^{-32}	4.97×10^{23} years	8.50×10^{-151}	8.42×10^{-72}	2.61×10^{63} years
	300	1.53×10^{-7}	1.99×10^{-7}	40.3 day	1.91×10^{-14}	9.31×10^{-14}	2.36×10^{5} years

[a] Calculated at the AE-CCSD(T)/aVTZ//AE-MP2/aVTZ level of theory.

300 K, and in both cases, only forward reactions are possible even on the molecular cloud time scale. For example, at 300 K, the half-lives of $HOCH_2CH_2O^{\cdot}$ and $HO^{\cdot}CHCH_2OH$ are 40.3 days and 2.36×10^5 years, respectively.

(5) A similar H-tunnelling scenario as that outlined in 4 (above) pertains for the system $CH_3NH^{\cdot}/{}^{\cdot}CH_2NH_2$ except that the half-lives of the forward and reverse reactions at 300 K are 73 and 2.75×10^7 years, respectively. Thus interconversion between these radicals is of low probability in the interstellar medium.

(6) This theoretical study shows that quantum mechanical H-tunnelling effects are very large at temperatures approaching 0 K for the chosen 1,2, 1,3 and 1,4 intramolecular H transfer reactions. Except in the case of the isomerisation of ${}^{\cdot}CH_2SH$ to $CH_3S^{\cdot}$, the k_{WKB} rates are too slow at low temperatures for the reactions to proceed even though H-tunnelling is pronounced. In all the studied cases, H-tunnelling decreases as the temperature increases, this behaviour is in agreement with previous reports.[28–32] In some cases k_{CVT} approaches k_{WKB} as the temperature approaches 300 K. At 300 K, with the exception of $CH_3NH^{\cdot}$, k_{WKB} rates (which include the H-tunnelling contributions) are high enough to permit the rearrangement to proceed, albeit it slowly in some instances.

(7) The WKB method has been found to be applicable to all of the studied systems. The Eckart method (see ESI†) is satisfactory for three of the systems, but significantly underestimates the width of the barrier in the systems $CH_3CO_2^{\cdot}/{}^{\cdot}CH_2CO_2H$ and $HOCH_2CH_2O^{\cdot}/HO^{\cdot}CHCH_2OH$. Thus, for these two systems, the Eckart method predicts H-tunnelling effects higher than those estimated using the WKB method.

Computational methods

Electronic structure calculations

The geometries of the relevant stationary points for all reactions investigated here were optimised at the all-electron (AE) unrestricted second-order Møller–Plesset perturbation theory (UMP2)[53,54] in conjunction with basis set aug-cc-pVTZ,[55] employing analytical gradient procedures. All the stationary points were characterised by their harmonic vibrational frequencies as minima or saddle points. The minima connected by a given transition structure were confirmed by intrinsic reaction coordinate (IRC)[56] calculations also at AE-MP2/aug-cc-pVTZ level of theory. Zero-point vibrational energies (ZPVEs) were determined from the harmonic vibrational frequencies calculated.

Single-point electronic energy calculations were treated using all-electron coupled-cluster calculations including all single and double excitations, together with a perturbative treatment of all connected triple excitations, designated CCSD(T),[50] were carried

Table 6 Summary of tunnelling effects at 50 and 300 K in the five studied systems

Isomerisation	Turning Point at 0 K (amu$^{1/2}$ bohr)	T (K)	Forward			Reverse		
			k_{CVT} (s^{-1})	k_{WKB} (s^{-1})	Half-life (WKB)	k_{CVT} (s^{-1})	k_{WKB} (s^{-1})	Half-life (WKB)
$^{\cdot}CH_2SH$ to $CH_3S^{\cdot}$[a]	(−1.59, 1.15)	50	4.76×10^{-88}	2.86×10^{-6}	67.2 h	9.97×10^{-150}	3.00×10^{-71}	7.33×10^{62} years
		300	2.92×10^{-4}	1.29×10^{-2}	53.7 s	2.49×10^{-14}	5.70×10^{-13}	3.86×10^{4} years
$CH_3O^{\cdot}$ to $^{\cdot}CH_2OH$[a]	(−1.51, 1.19)	50	3.04×10^{-118}	4.44×10^{-8}	180.6 day	1.00×10^{-143}	4.49×10^{-35}	4.89×10^{26} years
		300	2.43×10^{-9}	1.32×10^{-5}	14.6 h	1.18×10^{-13}	1.12×10^{-9}	19.6 years
$CH_3CO_2^{\cdot}$ to $^{\cdot}CH_2CO_2H$[b]	(−2.87, 1.95)	50	1.74×10^{-109}	4.91×10^{-18}	4.48×10^{9} years	1.00×10^{-126}	2.06×10^{-34}	1.07×10^{26} years
		300	6.71×10^{-8}	7.86×10^{-7}	245.0 h	4.45×10^{-10}	8.89×10^{-10}	24.7 years
$HOCH_2CH_2O^{\cdot}$ to $HO^{\cdot}CHCH_2OH$[b]	(−5.84, 1.45)	50	2.79×10^{-108}	4.42×10^{-32}	4.97×10^{23} years	8.50×10^{-151}	8.42×10^{-72}	2.61×10^{63} years
		300	1.53×10^{-7}	1.99×10^{-7}	40.3 day	1.91×10^{-14}	9.31×10^{-14}	2.36×10^{5} years
$CH_3{}^{\cdot}NH$ to $^{\cdot}CH_2NH_2$[a]	(−1.74, 1.49)	50	3.36×10^{-148}	6.42×10^{-14}	3.42×10^{5} years	1.44×10^{-179}	2.99×10^{-47}	7.34×10^{38} years
		300	1.67×10^{-14}	3.01×10^{-10}	73.0 years	3.42×10^{-19}	7.99×10^{-16}	2.75×10^{7} years

[a] Calculated at AE-CCSD(T)/aVQZ//AE-MP2/aVTZ level of theory. [b] Calculated at AE-CCSD(T)/aVTZ//AE-MP2/aVTZ level of theory.

out with the correlation consistent aug-cc-pVnZ basis sets, where n equals to D, T and Q.[55] For simplicity, these basis sets are denoted as aVnZ hereafter. The AE-CCSD(T) energies were extrapolated to the complete basis set (CBS) limit energies using standard form as follows[57]

$$E(x) = A_{CBS} + B\ \exp[-(x-1)] + C\ \exp[-(x-1)^2] \quad (1)$$

where x = 2, 3 and 4, corresponding to n = D, T and Q in the aVnZ, respectively.

The single-point energies for the intrinsic reaction coordinate (IRC) were carried out at AE-CCSD(T)/aVQZ (for $CH_3{}^{\cdot}NH$, $CH_3O^{\cdot}$ and $^{\cdot}CH_2SH$ isomerisations) or AE-CCSD(T)/aVTZ (for $CH_3CO_2^{\cdot}$ and $HOCH_2CH_2O^{\cdot}$ isomerisations) level. All of these calculations were performed with the GAUSSIAN 09[58] suite of programs. Using canonical variational transition state theory (CVT) to evaluate rate constants has been described elsewhere.[59]

Tunnelling analysis

Two different approaches were employed to investigate the tunnelling effect for each system under investigation, namely, WKB (Wentzel–Kramers–Brillouin)[60] and Eckart[61–63] methods. The WKB method computes the tunnelling contribution to the rate within a reaction-path Hamiltonian model by multiplying the classical rate at which the reactant hits the reaction barrier by the quantum mechanical transmission probability. This procedure requires the reaction path (potential energy as a function of reaction coordinate) to be determined at a high level of theory (see Section 1 above). The final potential energies correspond to the sum of AE-CCSD(T)/aVQZ or AE-CCSD(T)/aVTZ energy of IRC and ZPVEs (modes orthogonal to the path). Then, the potential energy function $V(s)$ in terms of the arc length s (atomic units) in mass-weighted coordinates along the H transfer IRC was fitted with a polynomial expression. The order of the expression was determined to make the potential energy $V(s)$ extended smoothly all the way to the minima. Tunnelling probabilities [$P(\varepsilon)$] were evaluated by computing one-dimensional barrier penetration integrals [$\theta(s)$] numerically along the potential energy curve and invoking the standard WKB formula:

$$\theta(\varepsilon) = \frac{1}{\hbar}\int_{s_1}^{s_2} \sqrt{2\mu[V(s)-\varepsilon]}\ \mathrm{d}s \quad (2)$$

$$P(\varepsilon) = \frac{1}{1+\mathrm{e}^{2\theta(\varepsilon)}} \quad (3)$$

where ε is the collision energy, μ is the corresponding reduced mass, s is the reaction coordinate, s_1 and s_2 are the turning points where the $V(s) = \varepsilon$.

The tunnelling rate constant at a energy ε is then

$$k_{WKB} = \frac{\omega_0}{2\pi}P(\varepsilon) = \frac{\omega_0}{2\pi}\frac{1}{1+\exp\left(-\frac{2}{\hbar}\int_{s_2}^{s_1}\sqrt{2\mu[V(s)-\varepsilon]}\,\mathrm{d}s\right)} \quad (4)$$

where ω_0 is the vibrational "reaction" mode of reactant that leads toward transition state.

The temperature dependent rate constant expression including the Boltzmann population of different vibrational levels is as follows,

$$k(T) = \frac{\sum_{n=0}^{\infty} k(n\hbar\omega_0)\mathrm{e}^{-(n\hbar\omega_0/kT)}}{\sum_{n=0}^{\infty}\mathrm{e}^{-(n\hbar\omega_0/kT)}} \quad (5)$$

in which T is the temperature. The results from Eckart method are discussed in the ESI.†

The half-life $\tau_{1/2}$ is determined by the following equation,

$$\tau_{1/2} = \frac{\ln 2}{k(T)} \quad (6)$$

Acknowledgements

This project was funded by the Australian Research Council. TW thanks the ARC for a research associateship stipend. We thank eResearch (The University of Adelaide) and the Australian Partnership for Advanced Computing (Australian National University) for generous allocations of supercomputing time.

Notes and references

1 G. E. R. Lloyd, *Aristotle: The Growth and Structure of his Thought*, Cambridge University Press, Cambridge, UK, 1968, pp. 133–139.
2 http://www.astro.uni-koeln.de/cdms/molecules
3 http://www.astrochymist.org/astrochymist_ism.html
4 I. W. Smith, *Annu. Rev. Astron. Astrophys.*, 2011, **49**, 29.
5 T. P. Snow and V. M. Bierbaum, *Annu. Rev. Anal. Chem.*, 2008, **1**, 229.
6 Y. J. Kuan, S. B. Charnley, H. C. Huang, W. L. Tseng and Z. Kisiel, *Astrophys. J.*, 2003, **593**, 848.
7 O. Botta, Z. Martins, C. Emmenegger, J. P. Dworkin, D. P. Glavin, R. P. Harvey, R. Zenobi, J. L. Bada and P. Ehrenfreund, *Meteorit. Planet. Sci.*, 2008, **43**, 1465.
8 O. Botta, Z. Martins, C. Emmenegger, J. P. Dworkin, D. P. Glavin, R. P. Harvey, R. Zenobi and P. Ehrenfreund, *Meteorit. Planet. Sci.*, 2006, **41**, A26.
9 W. H. Sorrell, *Astrophys. J.*, 2001, **555**, L129.
10 P. D. Holtom, C. J. Bennett, Y. Osamura, N. J. Mason and R. I. Kaiser, *Astrophys. J.*, 2005, **626**, 940.
11 D. J. Knowles, T. Wang and J. H. Bowie, *Org. Biomol. Chem.*, 2010, **8**, 4934.
12 D. M. Mehringer, L. E. Snyder and Y. T. Miao, *Astrophys. J.*, 1997, **480**, L71.
13 D. T. Halfen, A. J. Apponi, N. Woolf, R. Polt and L. M. Ziurys, *Astrophys. J.*, 2006, **639**, 237.
14 J. M. Hollis, F. J. Lovas and P. R. Jewell, *Astrophys. J.*, 2000, **540**, L107.
15 G. Flanagan, S. N. Ahmed and P. B. Shevlin, *J. Am. Chem. Soc.*, 1992, **114**, 3892.
16 V. G. Kiselev, S. Swinnen, V. S. Nguyen, N. P. Gritsan and M. T. Nguyen, *J. Phys. Chem. A*, 2010, **114**, 5573.
17 P. R. Schreiner and H. P. Reisenauer, *ChemPhysChem*, 2006, **7**, 880.
18 T. Wang and J. H. Bowie, *Org. Biomol. Chem.*, 2010, **8**, 4757.
19 A. F. Jalbout, L. Abrell, L. Adamowicz, R. Polt, A. J. Apponi and L. M. Ziurys, *Astrobiology*, 2007, **7**, 433.
20 T. P. M. Goumans and J. Kastner, *J. Phys. Chem. A*, 2011, **115**, 10767.
21 T. I. Hasegawa and E. Herbst, *Mon. Not. R. Astron. Soc.*, 1993, **261**, 83.
22 K. Hiraoka, T. Sato and T. Takayama, *Science*, 2001, **292**, 869.
23 B. Y. Welsh, J. V. Vallerga and K. McDonald, *Publ. Astron. Soc. Pac.*, 1998, **110**, 827.
24 D. Gerbig, H. P. Reisenauer, C. H. Wu, D. Ley, W. D. Allen and P. R. Schreiner, *J. Am. Chem. Soc.*, 2010, **132**, 7273.
25 P. R. Schreiner, H. P. Reisenauer, D. Ley, D. Gerbig, C. H. Wu and W. D. Allen, *Science*, 2011, **332**, 1300.
26 P. R. Schreiner, H. P. Reisenauer, F. C. Pickard, A. C. Simmonett, W. D. Allen, E. Matyus and A. G. Csaszar, *Nature*, 2008, **453**, 906.
27 T. Wang and J. H. Bowie, *Org. Biomol. Chem.*, 2012, **10**, 652.
28 M. J. S. Dewar, K. M. Merz and J. J. P. Stewart, *J. Chem. Soc., Chem. Commun.*, 1985, 166.
29 D. Gerbig, D. Ley and P. R. Schreiner, *Org. Lett.*, 2011, **13**, 3526.
30 R. A. Moss, R. R. Sauers, R. S. Sheridan, J. Z. Tian and P. S. Zuev, *J. Am. Chem. Soc.*, 2004, **126**, 10196.
31 G. R. Shelton, D. A. Hrovat and W. T. Borden, *J. Am. Chem. Soc.*, 2007, **129**, 164.
32 P. S. Zuev, R. S. Sheridan, T. V. Albu, D. G. Truhlar, D. A. Hrovat and W. T. Borden, *Science*, 2003, **299**, 867.
33 P. Ehrenfreund and S. B. Charnley, *Annu. Rev. Astron. Astrophys.*, 2000, **38**, 427.
34 P. Ehrenfreund, W. Irvine, L. Becker, J. Blank, J. R. Brucato, L. Colangeli, S. Derenne, D. Despois, A. Dutrey, H. Fraaije, A. Lazcano, T. Owen and F. Robert, *Rep. Prog. Phys.*, 2002, **65**, 1427.
35 D. Antoniou, S. Caratzoulas, C. Kalyanaraman, J. S. Mincer and S. D. Schwartz, *Eur. J. Biochem.*, 2002, **269**, 3103.
36 J. P. Bothma, J. B. Gilmore and R. H. McKenzie, *New J. Phys.*, 2010, **12**, 055002.
37 M. J. Knapp and J. P. Klinman, *Eur. J. Biochem.*, 2002, **269**, 3113.
38 S. Q. Machleder, J. Pineda and S. D. Schwartz, *J. Phys. Org. Chem.*, 2010, **23**, 690.
39 Z. D. Nagel and J. P. Klinman, *Chem. Rev.*, 2006, **106**, 3095.
40 K. S. Peters, *Acc. Chem. Res.*, 2009, **42**, 89.
41 L. E. Snyder, J. M. Hollis and B. L. Ulich, *Astrophys. J.*, 1976, **208**, L91.
42 J. A. M. Simoes, A. Greenberg and J. F. Liebman, *Energetics of Organic Free Radicals*, Blackie Academic & Professional, London, 1st edn, 1996.
43 T. C. Mouschovias, K. Tassis and M. W. Kunz, *Astrophys. J.*, 2006, **646**, 1043.
44 K. Tassis and T. C. Mouschovias, *Astrophys. J.*, 2004, **616**, 283.
45 K. M. Downard, J. C. Sheldon, J. H. Bowie, D. E. Lewis and R. N. Hayes, *J. Am. Chem. Soc.*, 1989, **111**, 8112.
46 http://webbook.nist.gov/chemistry/
47 R. T. Bise, H. Choi, H. B. Pedersen, D. H. Mordaunt and D. M. Neumark, *J. Chem. Phys.*, 1999, **110**, 805.
48 J. M. Nicovich, K. D. Kreutter, C. A. Vandijk and P. H. Wine, *J. Phys. Chem.*, 1992, **96**, 2518.
49 S. G. Lias, J. E. Bartmess, J. F. Liebman, J. L. Holmes, R. D. Levin and W. G. Mallard, *J. Phys. Chem. Ref. Data*, 1988, **17**, 1.
50 D. F. McMillen and D. M. Golden, *Annu. Rev. Phys. Chem.*, 1982, **33**, 493.
51 B. K. Janousek, K. J. Reed and J. I. Brauman, *J. Am. Chem. Soc.*, 1980, **102**, 3125.
52 J. H. Bowie and S. Dua, in *Encyclopaedia of Spectroscopy and Spectrometry*, ed. J. C. Lindon, G. E. Tranter and J. L. Holmes, Academic Press, London, 1999, vol. 1, p. 1461.
53 J. M. Bofill, *J. Comput. Chem.*, 1994, **15**, 1.
54 H. B. Schlegel, *J. Comput. Chem.*, 1982, **3**, 214.
55 T. H. Dunning, *J. Chem. Phys.*, 1989, **90**, 1007.
56 K. Fukui, *Acc. Chem. Res.*, 1981, **14**, 363.
57 K. A. Peterson, D. E. Woon and T. H. Dunning, *J. Chem. Phys.*, 1994, **100**, 7410.
58 M. J. Frisch, G. W. Trucks, H. B. Schlegel, G. E. Scuseria, M. A. Robb, J. R. Cheeseman, G. Scalmani, V. Barone, B. Mennucci, G. A. Petersson, H. Nakatsuji, M. Caricato, X. Li, H. P. Hratchian, A. F. Izmaylov, J. Bloino, G. Zheng, J. L. Sonnenberg, M. Hada, M. Ehara, K. Toyota, R. Fukuda, J. Hasegawa, M. Ishida, T. Nakajima, Y. Honda, O. Kitao, H. Nakai, T. Vreven, J. Montgomery, J. A. J. E. Peralta, F. Ogliaro, M. Bearpark, J. J. Heyd, E. Brothers, K. N. Kudin, V. N. Staroverov, R. Kobayashi, J. Normand, K. Raghavachari, A. Rendell, J. C. Burant, S. S. Iyengar, J. Tomasi, M. Cossi, N. Rega, N. J. Millam, M. Klene, J. E. Knox, J. B. Cross, V. Bakken, C. Adamo, J. Jaramillo, R. Gomperts, R. E. Stratmann, O. Yazyev, A. J. Austin, R. Cammi, C. Pomelli, J. W. Ochterski, R. L. Martin, K. Morokuma, V. G. Zakrzewski, G. A. Voth, P. Salvador, J. J. Dannenberg, S. Dapprich, A. D. Daniels, Ö. Farkas, J. B. Foresman, J. V. Ortiz, J. Cioslowski and D. J. Fox, *GAUSSIAN 09*, Gaussian Inc., Wallingford, CT, 2009.
59 D. G. Truhlar and B. C. Garrett, *Annu. Rev. Phys. Chem.*, 1984, **35**, 159.
60 L. D. Landau and E. M. Lifshitz, *Quantum Mechanics: Non-Relativistic Theory*, Pergamon Press, Oxford, New York, 3rd edn, 1977.
61 C. Eckart, *Phys. Rev.*, 1930, **35**, 1303.
62 H. S. Johnston and J. Heicklen, *J. Phys. Chem.*, 1962, **66**, 532.
63 T. N. Truong and D. G. Truhlar, *J. Chem. Phys.*, 1990, **93**, 1761.